(27) Wunderlich, B. *Macromolecular Physics*; Academic Press: New York, 1980; Vol. 3.
(28) Yano, S. *J. Polym. Sci. A-2* **1970**, *8*, 1057. Yano, S.; Tadano, K.; Aoki, K. Koizumi, N. *J. Polym. Sci., Polym. Phys. Ed.* **1974**, *12*, 1875.
(29) Paul, D. R.; Altamirano, J. O. *Adv. Chem. Ser.* **1975**, *142*, 371.
(30) Hirata, Y.; Kotaka, T. *Polym. J.* **1981**, *13*, 273.
(31) Morra, B. S.; Stein, R. S. *Polym. Eng. Sci.* **1984**, *24*, 311.
(32) Murali, R.; Eisenberg, A. *J. Polym. Sci., Part B: Polym. Phys.* **1988**, *26*, 1385.

Kinetics of Phase Separation of Perfluorinated Nafion Ionomer and Poly(vinylidene fluoride) Blends

Jen-Chang Yang and Thein Kyu*

Center for Polymer Engineering, University of Akron, Akron, Ohio 44325.

Received March 10, 1989; Revised Manuscript Received June 6, 1989

ABSTRACT: Liquid–liquid phase separation was observed in the blends of Nafion and poly(vinylidene fluoride) (PVDF) above the crystal melting temperature of PVDF crystals. The kinetics of thermally induced phase separation in Nafion/PVDF blends was investigated by means of time-resolved small-angle light scattering. A temperature–composition phase diagram was established on the basis of cloud point measurements. The phase behavior is a lower critical solution temperature (LCST) type and reversible in character. Temperature-jump (*T*-jump) experiments were undertaken from room temperature to 220 and 240 °C. Phase separation was dominated by the late stages of spinodal decomposition. The time evolution of scattering curves was analyzed in the context of nonlinear theories and dynamic scaling laws.

Introduction

In a previous paper,[1] the effects of solvent casting on the development of spherulitic structure of poly(vinylidene fluoride) (PVDF) and the morphology of its blend with Nafion have been demonstrated. We found that the formation of α- or γ-form or mixed α- and γ-form crystals strongly depends on the temperature of solvent casting and blend compositions. The existence of a crystalline structure in the Nafion/PVDF blends makes the determination of polymer miscibility very difficult. However, the dielectric relaxation study showed a systematic movement of the α relaxation peak with composition, implying that the polymer pair may be, at least, partially miscible in the solid state. When the blend system was heated above the crystal melting temperature of PVDF, liquid–liquid phase separation took place.

In the present study, we continue our efforts to elucidate the dynamics of liquid–liquid phase separation by using time-resolved light scattering. We first establish the cloud point phase diagram. A couple of temperature jumps (*T* jumps) were carried out from room temperature to a two-phase region (220 and 240 °C) to investigate kinetics of phase separation.

Experimental Section

Nafion membranes in the acid form (N 117, equivalent weight $\cong$ 1100) were supplied by Du Pont and PVDF (KF 1000, $M_w \cong$ 282 000 and $M_w/M_n = 1.8$) was obtained from Kureha Chemical Co. They were dissolved separately in 1-methyl-2-pyrrolidinone (NMP) by rigorous stirring at 120 °C and room temperature, respectively. The solutions were subsequently mixed at 1 wt % polymer concentration in various blend compositions. Blend films were cast on microscope glass slides at 60 °C in an air oven. The average thickness of the specimens was about 10 μm.

Light scattering intensity scans were acquired on a time-resolved light scattering setup described previously.[2] A He-Ne laser (2 mW) with a wavelength of 632.8 nm was used as a light source. A set of sample hot stages was utilized for *T*-jump experiments; one is controlled at the experimental temperature and the other is used for preheating. In the present study, a second heating block was not used, as the *T*-jump experiments were carried out from room temperature to 220 and 240 °C. The scattered intensity was measured by means of a two-dimensional camera (Model 1252 B, EG & G Princeton Applied Research Co.) interfaced with an optical multichannel analyzer (OMA III, Model 1460, EG & G Co.). The data analysis, such as background subtraction, smoothing, rescaling, etc., was carried out on an off-line microcomputer (IBM-PC). Light scattering pictures were obtained by using a Polaroid instant camera (Land film holder, Model 545). Optical micrographs were photographed on a Leitz microscope (Laborlux Pol-12).

Results and Discussion

As mentioned previously,[1] thermally induced phase separation takes place during heating above the melting temperature (T_m) of PVDF crystals. Figure 1 shows a scattering halo of the 40/60 Nafion/PVDF blend at 230 °C, arising from the periodic concentration fluctuations of phase-separated domains. The optical microscopic investigation reveals interconnected domain structures, which are the familiar characteristics of spinodal decomposition (SD). SD is a spontaneous process that is extremely unstable at infinitesimal concentration fluctuations.[3,4] An alternative mechansim is nucleation and growth (NG), which is stable at small fluctuations but is unstable at large composition fluctuations. In the latter process, a stable nucleus forms first and the phase-separated domains grow subsequently. If this process were to occur, a component of scattering should decrease from a maximum at $q = 0$, which is not seen here. In other words, liquid–liquid phase separation occurs through SD rather than NG.[3,4]

---

* To whom correspondence should be addressed.

0024-9297/90/2223-0182$02.50/0

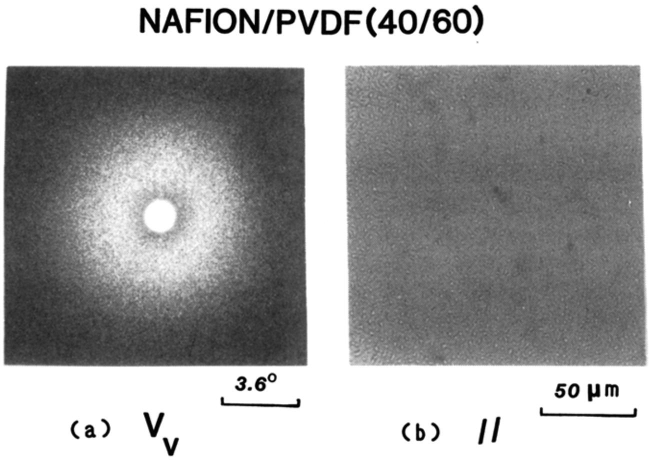

Figure 1. Interconnected structure of 40/60 Nafion/PVDF blends and the corresponding halo during liquid-liquid phase separation at 230 °C.

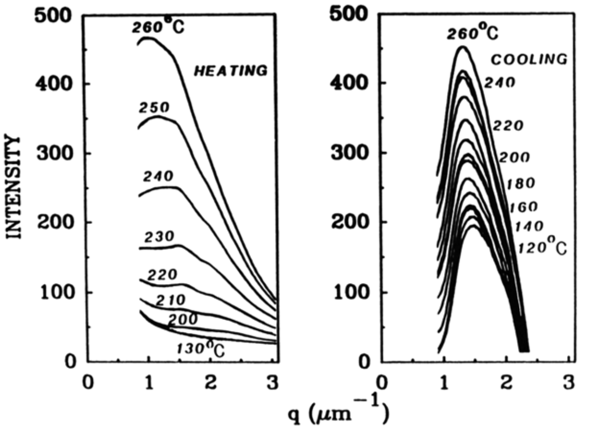

Figure 2. Evolution of V_v scattering curves during heating and cooling of 40/60 Nafion/PVDF.

The evolution of the V_v (vertical polarizer with vertical analyzer) scattering curves during heating and cooling of 60/40 Nafion/PVDF is shown in Figure 2. The peak maximum first appears at around 200 °C and then moves to a lower scattering angle with continued heating. This may be attributed to phase growth. Upon cooling from 260 °C, the scattered intensity decays gradually without accompanying any movement of the peak position, suggesting the dissolution of phase domains. When the temperature reaches about 150 °C, crystallization of PVDF takes place, resulting in an increase in the scattered intensity. This observation suggests that the phase-separation process may be a reversible one. A similar observation was also made in the blends of Nafion–Na$^+$ salt and PVDF, which is not shown here.[5] Both acid and salt Nafion blends show no indication of thermal degradation.

Figure 3 shows the variation of scattered intensity at a scattering angle $\theta \sim 20°$ with temperature for 40/60 Nafion/PVDF. The initial increase in the scattered intensity near 150 °C is due to the annealing effect. The onset of the intensity reduction occurs at around 175 °C, probably associated with the premelting of PVDF crystals, and the melting is completed in the vicinity of 185 °C. The intensity increases again with further increase of temperature, which may be attributed to liquid–liquid phase separation of Nafion/PVDF mixtures. The determination of the cloud point from such temperature dependence of intensity is ambiguous. Thus, an attempt was made to eliminate the effect of crystal melting; i.e., the specimen was heated at 200 °C for 10 min, then cooled gradually to 155 °C, and kept there for 30 min. The blend specimen was again subjected to a second heating cycle. The temperature dependence of scattered intensity of the second heating run is shown in Figure 4. The curve reveals a familiar trend normally observed in the determination of the cloud point temperature of amorphous polymer blends.[3] The cloud point temperature versus composition phase diagram of Nafion/PVDF obtained at a heating rate of 0.2 °C/min is depicted in Figure 5. The phase behavior is an LCST type with a minimum at the 60/40 composition and at 187 °C, suggesting that liquid–liquid phase separation takes place above the T_m of PVDF crystals. Since, liquid–liquid phase separation is a kinetic process, it depends on heating rates. Figure 6 exhibits the dependence of the cloud point temperature on heating rates. It should be borne in mind that the slow heating rate data may be affected by the contribution from the kinetic process. Such effects may be small at fast heating rates. However, the equilibrium cloud point is generally overestimated at high heating rates, and thus it generally appears at a higher temperature. Hence, the exact binodal point is difficult to determine from such nonequilibrium studies.

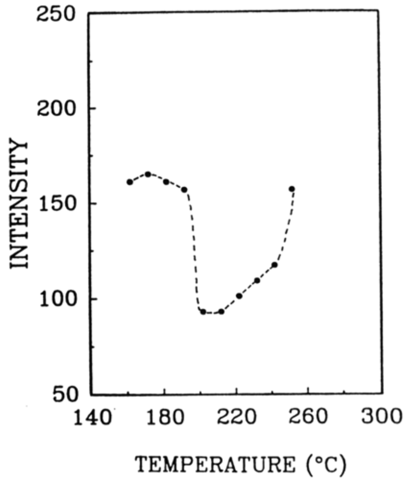

Figure 3. Temperature dependence of scattered intensity ($\theta \sim 20°$) for 40/60 Nafion/PVDF in the first heating run.

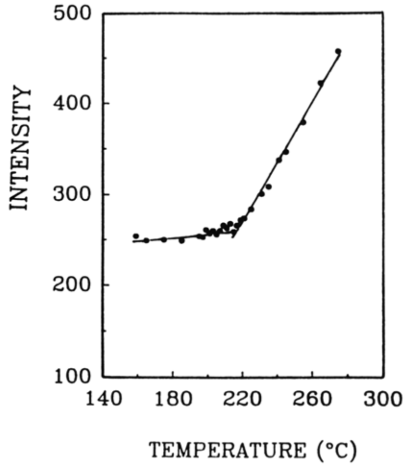

Figure 4. Temperature dependence of scattered intensity ($\theta \sim 20°$) for 40/60 Nafion/PVDF in the second run, after cooling down to 155 °C from 200 °C.

Now, we turn our attention to the kinetic study. Figure 7 shows the time evolution of scattering curves of 60/40 Nafion/PVDF blends, following T jumps from room temperature to 220 and 240 °C. The scattering maxi-

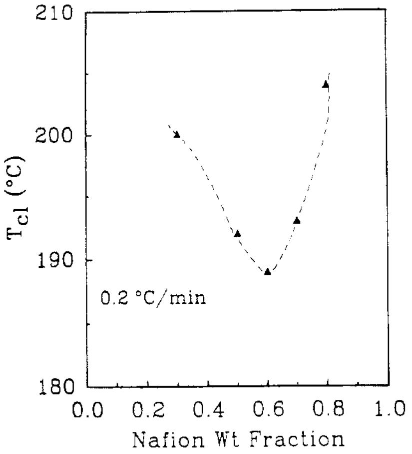

Figure 5. Cloud point phase diagram of Nafion/PVDF at a heating rate of 0.2 °C/min.

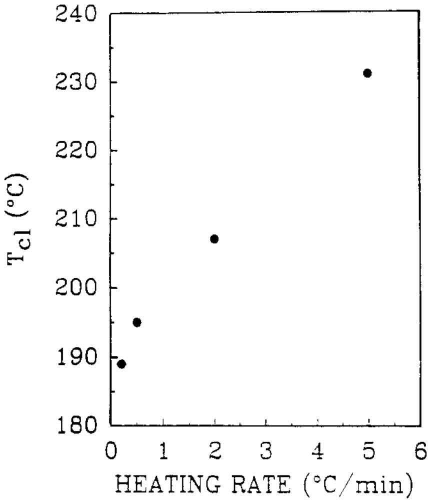

Figure 6. Heating rate dependence of the cloud point temperature for 60/40 Nafion/PVDF.

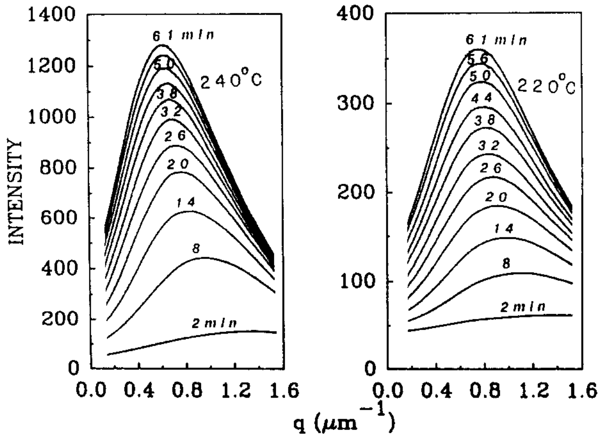

Figure 7. Time evolution of scattering curves of 60/40 Nafion/PVDF blends, following T jumps from room temperature to 220 and 240 °C.

mum appears around a wavenumber of 1.8 (1/μm) and then gradually moves to lower wavenumbers. The linear regime in the early stage of SD has not been observed; i.e., there is no period at which the scattering peak remains stationary.[6,7] Therefore, it may be concluded that the phase separation in Nafion/PVDF blends is governed by the coarsening process and is nonlinear in character.[8] It should be pointed out that the initial maximum wavenumber is more or less the same as the scattering peak of PVDF spherulites. It seems the moment spherulites melt, phase separation takes place. There is no sufficient time for homogenization of phases to occur, therefore the initial concentration fluctuation size turns out to be large. We are probably looking at the growth process, i.e., the late stages of spinodal decomposition.

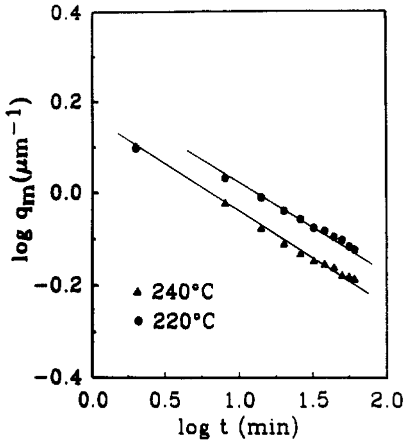

Figure 8. log–log plots of maximum wavenumber versus phase separation time for 60/40 Nafion/PVDF at 220 and 240 °C.

The late stages of SD was treated by Langer, Baron, and Miller (LBM)[8] on the basis of the nonlinear statistical theory. The LBM theory predicts a power law scheme rather than an exponential growth. Binder and Stauffer (BS)[9] reached a similar formulation on the basis of the cluster theory, in which the clusters aggregate and coalesce to larger domains associated with a decrease in free energy of the system. Both theories suggest that the maximum wavenumber $q_m(t)$ has a simple form of the power law

$$q_m(t) \sim t^{-\varphi} \tag{1}$$

and

$$I_m(t) \sim t^{\psi} \tag{2}$$

where q is defined as $q = (4\pi/\lambda) \sin \theta/2$ in which λ and θ are the wavelength of incident light and a scattering angle measured in the medium. Here, the exponents φ and ψ are predicted to have the relationship $3\varphi = \psi$, but with different values. Langer, Baron, and Miller[8] estimated a value of $\varphi = 0.21$ from their nonlinear calculation. Binder and Stauffer[9] predicted $\varphi = 1/3$ and $\psi = 1$ on the basis of the cluster dynamics, i.e., the coalescence of phase domains. Siggia[10] suggested a value of $\varphi = 1/3$ at the early growth regime, and this varies with a slope of −1 at intermediate stages where the percolation process takes place. On the other hand, Kawasaki and Ohta,[11] who took into consideration hydrodynamic effects, concluded that there is no scaling law for the entire phase separation process.

Figure 8 shows log–log plots of q_m versus t for 60/40 Nafion/PVDF blends. The slopes are approximately −0.18 to −0.20. The corresponding maximum intensity $I_m(t)$ was plotted against t on a logarithmic scale in Figure 9. Depending on the T jumps, the values of ψ are in the range 0.53–0.58. According to Binder,[12] the exponent φ varies with a $1/(d + 2)$ power for the bulk mobility and $1/(d + 3)$ for the surface mobility, where the thermal fluctuation is dominant and d is the dimensionality of growth. Hence, an observed value of 1/5 has been predicted by LBM[8] and Binder.[12] Very recently, Furukawa[13] proposed a general scaling for kinetic exponents to vary as $1/(d + 2 + \zeta - h)$ in order to describe various crossover processes. The two new parameters ζ and h

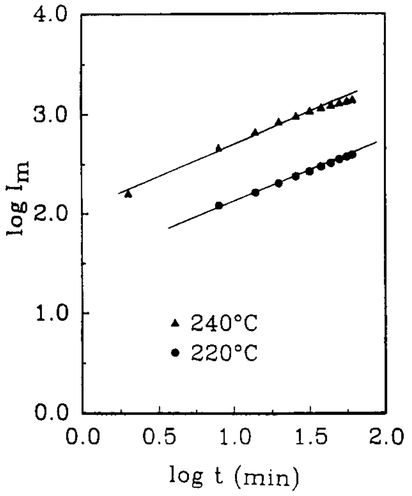

Figure 9. Corresponding maximum intensity versus phase separation time in log–log plots.

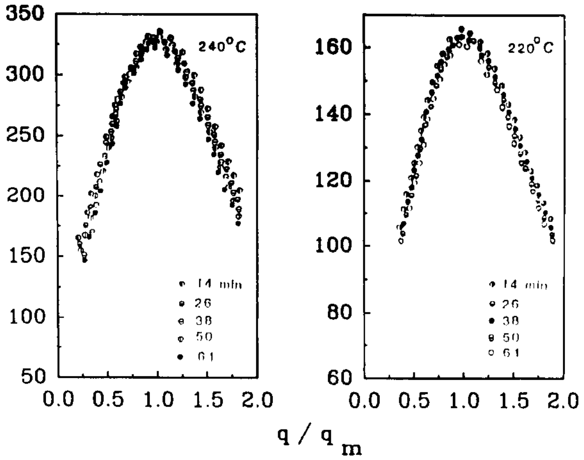

Figure 10. Plots of $I(q)q_m^3$ versus q/q_m for self-similarity tests.

may assume different values depending on which growth mechanism is dominant.[12,13]

Now we shall examine the time evolution of a scattering function in terms of a scaling law for self-similarity between the phase structures.[14] The scattered intensity at a given time t may be related to the scaled structure function $s(z)$ as follows:

$$I(q,t) \sim V\langle\eta^2\rangle\xi(t)^3 s(z) \tag{3}$$

where V is the irradiated volume, $\langle\eta^2\rangle$ is the mean-square fluctuations of refractive indices, and $z = q\xi(t)$. Here, $\xi(t)$ is the correlation length which is related to the wavelength of the periodic structure $\Lambda(t)$ by the following equation:

$$\xi(t) = \Lambda(t)/2\pi = 1/q_m(t) \tag{4}$$

In the region where $\langle\eta^2\rangle$ is constant, the structure factor $s(z)$ can be described as

$$s(z) \sim I(q,t)q_m^{\ 3}(t) \tag{5}$$

This scaling prediction has been tested for time evolution of scattering data of 60/40 Nafion/PVDF blends. As can be seen in Figure 10, the plots of $I_m(q)q_m^{\ 3}$ versus q/q_m give fairly good superposed master curves, suggesting self-similarity in the demixing process. Temporal self-similarity is generally obtained when the structure function becomes universal with time.

Another scaling theory that is of interest is due to Furukawa[15] who proposed that the shape of the structure function can be scaled by the following equation:

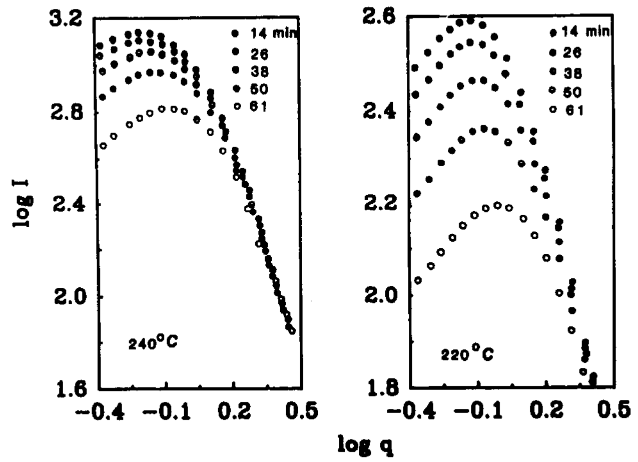

Figure 11. Shapes of scaled scattering function for 60/40 Nafion/PVDF blends.

$$s(x) = \frac{(1 + \gamma/2)x^2}{\gamma/2 + x^{2+\gamma}} \tag{6}$$

where $x = qR$ with R the diameter of the domain. γ is predicted to be equal to $2d$ for a critical mixture and $(d + 1)$ for off-critical mixtures, and d is the dimensionality of fluctuation growth. In the region of $q < q_m$, the structure function $s(q,t)$ has the form

$$s(x) \sim x^2 \tag{7}$$

whereas in the large q region where $q > q_m$, we have

$$s(x) \sim x^{-\gamma} \tag{8}$$

If it is a three-dimensional growth, γ will be 6 and 4 for the critical and off-critical mixtures, respectively. In the case of two-dimensional growth, the values of γ will be 4 and 3.

Figure 11 shows log–log plots of $I(q,t)$ versus q for 60/40 Nafion/PVDF mixtures. In the region of $q < q_m$, the slopes are slightly smaller than the predicted value of 2. The incomplete elimination of a parasitic scattering at low scattering angles may be partly responsible for this discrepancy. At large q regions, the slopes of −4 were obtained for the 60/40 compositions. It is unclear whether the −4 slope represents the two-dimensional growth for the critical mixture or three-dimensional growth for off-critical compositions. Incidentally, the 60/40 Nafion/PVDF corresponds to the minimum composition in the cloud point curve in Figure 5, but it does not necessarily prove that it is the critical point. It should also be pointed out that the maximum wavenumber various from 1.4 to 0.6 (1/μm) during the course of phase separation, which corresponds to a fluctuation size of approximately 5–10 μm. In view of the thin Nafion/PVDF films (about 10 μm), it is plausible that the growth of concentration fluctuations may be close to a two-dimensional rather than a three-dimensional growth.

Conclusions

We observed liquid–liquid phase separation above the crystal melting temperature of PVDF crystals in mixtures of Nafion/PVDF. The cloud point phase diagram was established and similar in character with a lower critical solution temperature diagram. In the kinetic studies, the linear regime was not observed. The process of phase separation was dominated by the late stages of spinodal decomposition. Self-similarity was attained during the growth regime investigated and explained well by the dynamical scaling law.

Registry No. PVDF, 24937-79-9; N117, 119314-70-4.

References and Notes

(1) Kyu, T.; Yang, J. C. *Macromolecules*, preceding paper in this issue.
(2) Kyu, T.; Saldahna, J. M. *J. Polym. Sci., Polym. Lett. Ed.* **1988**, *26*, 33.
(3) Olabisi, O.; Robeson, L. M.; Shaw, M. T. *Polymer–Polymer Miscibility*; Academic: New York, 1979.
(4) Gunton, J. D.; San Miguel, M.; Sahni, P. S. In *Phase Transitions and Critical Phenomena*, Domb, C., Lebowitz, J. L., Eds.; Academic: New York, 1983; Vol. 8.
(5) Yang, J. C. M.S. Thesis, University of Akron, 1989.
(6) Cahn, J. W. *J. Chem. Phys.* **1965**, *42*, 93.
(7) Cahn, J. W.; Hilliard, J. E. *J. Chem. Phys.* **1958**, *28*, 258.
(8) Langer, J. S.; Baron, M.; Miller, H. D. *Phys. Rev. A* **1975**, *11*, 1417.
(9) Binder, K.; Stauffer, D. *Phys. Rev. Lett.* **1975**, *33*, 1006.
(10) Siggia, E. D. *Phys. Rev. A* **1979**, *20*, 595.
(11) Kawasaki, K.; Ohta, T. *Progr. Theor. Phys.* **1978**, *59*, 362.
(12) Binder, K.; Heermann, D. H. In *Scaling Phenomena in Disordered Systems*; Pynn, R., Skjeltorp, T., Eds.; Plenum: New York, 1985; p 207.
(13) Furukawa, H. *J. Appl. Crystallogr.* **1988**, *21*, 805.
(14) Furukawa, H. *Phys. Rev. Lett.* **1979**, *43*, 136.
(15) Furukawa, H. *Phys. A* **1984**, *123*, 497.

Optical Properties of Solvent-Cast Polymer Films

J. S. Machell, J. Greener,* and B. A. Contestable

Manufacturing Research and Engineering, Eastman Kodak Company, Rochester, New York 14650.

Received February 10, 1989; Revised Manuscript Received May 26, 1989

ABSTRACT: The optical properties of solvent-cast films were studied for several polymer formulations over a wide range of casting conditions. It is shown that the casting process induces distinct molecular order in the solid film as manifested by finite birefringence in the cross-film (transverse) direction. The optical anisotropy represents a random molecular alignment parallel to the film plane which can be observed only by measurements in oblique incidence. The level of birefringence depends on the general mode and conditions of the casting procedure and on the optical properties of the polymer. Two distinct procedures, free casting and blade casting, were evaluated and found to produce films with widely varied levels of birefringence. Birefringence was also influenced by the solvent type, the casting temperature, the surface energy of the substrate, and the timing of the peel-off step. In the limit of thin ($\lesssim 25$ μm) films, the transverse birefringence can be loosely correlated with the intrinsic birefringence of the polymer. Indeed, it is shown that by blending miscible polymers having intrinsic birefringences that are opposite in sign, one can produce effectively nonbirefringent films. Two such blends have been tested in this study. All our observations are interpreted in terms of a molecular "freezing-in" process induced by drying stresses.

I. Introduction

The optical properties of solvent-cast polymer films are of great technological importance in a host of optoelectronic systems and devices, e.g., in optical waveguides, in optical data storage systems, and in various linear and nonlinear optical components. These properties are generally dictated by the intrinsic optical anisotropy of the polymer chain and by the orientation induced during the casting operation. The alignment of polymer molecules and the corresponding optical anisotropy in solvent-cast films has been addressed by several investigators. General aspects of macromolecular organization in the vicinity of inorganic surfaces have been reviewed by Rickert et al.,[1] who consider in detail three features that control the behavior of polymer molecules near surfaces: (i) substrate properties, (ii) solution organization, and (iii) interfacial properties of macromolecules. All three features contribute, to some extent, to the level of molecular order near solid surfaces, and they underlie the complex nature of the corresponding phenomena.

Cherkasov et al.[2] studied orientation phenomena in polymer films produced by free casting (see next section for definition) and observed that the polymer molecules tend to align parallel to the solid surface in a manner resembling liquid-crystalline (cholesteric) order. They found, however, that the planar orientation has a finite range that depends on the stiffness of the polymer chain. For stiff backbone polymers the planar orientation zone may extend 20 μm into the film whereas for flexible chain polymers the high orientation zone is only ca. 1 μm thick. Some molecular order, according to Cherkasov et al., may extend well beyond this high orientation "skin" reaching 10–50 μm. Although the origin of this effect was not fully elucidated, it was speculated that the high orientation arises from steric/adhesion effects and long-range interactions of the solid surface with the polymer molecules.

Prest and Luca,[3,4] in a study on the properties of polymeric films cast from solution by thin, wire-wound, draw bars, also observed high planar orientation in the solid films. They view the molecular ordering process as a competition between planar conformation induced by drying ("drying stress") and the tendency of the molecules to drift toward a random ("equilibrium") conformation. As solvent evaporation proceeds, the molecular mobility in the collapsed film becomes increasingly restricted until the drying-induced conformations are "frozen" in the solid matrix as the glass transition is approached. Prest and Luca studied relatively thin films (1–5 μm) and evaluated the effects of solvent, polymer structure, molecular weight, and drying conditions on the birefringence level in the film. The contribution of drying stresses to the molecular organization in solvent-cast films was also noted by Sudduth and Rogers[5] and Sosnowski and Weber.[6] Cohen and Reich[7] studied the effects of molecular weight

0024-9297/90/2223-0186$02.50/0